Research Article Vol. 5, No. 10 / October 2018 / Optica 1322

Magnetic phase diagram of light-mediated spin structuring in cold atoms

G. Labeyrie,[1,*] I. Krešić,[2,3] G. R. M. Robb,[2] G.-L. Oppo,[2] R. Kaiser,[1] and T. Ackemann[2]

[1]Université Côte d'Azur, CNRS, Institut de Physique de Nice, Valbonne 06560, France
[2]SUPA and Department of Physics, University of Strathclyde, Glasgow G4 0NG, Scotland, UK
[3]Institute of Physics, Bijenička cesta 46, 10000 Zagreb, Croatia
*Corresponding author: guillaume.labeyrie@inphyni.cnrs.fr

Received 26 June 2018; revised 3 September 2018; accepted 8 September 2018 (Doc. ID 336137); published 18 October 2018

Self-organization in driven dissipative systems is an active field of research with implications in physics, chemistry, and biology. When applying a red-detuned retroreflected laser beam to a large cloud of cold atoms, we observe the spontaneous formation of 2D structures in the transverse plane corresponding to high contrast spatial modulations of both light field and atomic spins. By applying a weak magnetic field, we explore the rich resulting phase space and identify specific phases associated with both dipolar and quadrupolar terms of the atomic magnetic moment. In particular, we demonstrate spontaneous structures in optically induced ground state coherences representing magnetic quadrupoles. Our results illustrate the wealth of behavior exhibited by laser-driven atomic media with complex level structure under optical feedback.

OCIS codes: (190.4420) Nonlinear optics, transverse effects in; (270.3100) Instabilities and chaos; (270.1670) Coherent optical effects; (190.6135) Spatial solitons.

https://doi.org/10.1364/OPTICA.5.001322

1. INTRODUCTION

Since the first observation of the spontaneous appearance of hexagonal structures in the transverse cross section of laser beams counterpropagating in sodium vapor [1], self-organized optical structures have been investigated in various interaction geometries (cavities [2–8], single-mirror feedback arrangements [9–17], counterpropagating beams [9,18–22], hybrid systems such as liquid crystal light valves [23–25]), and many different nonlinear materials (liquid crystals [11,17], alkaline atoms [13,14,18,22], semiconductors [8], photorefractives [12,15]). These structures arise from the interaction of diffraction providing spatial coupling and optical nonlinearities. Analysis was mainly based on optical wave mixing mediated by the medium (e.g., explicitly in the class A limit in cavity transverse nonlinear optics [2,4,5] and in most treatments of counterpropagating beams [9,18,19]), although obviously there is always a corresponding structure in the matter variable the optical field is coupling to. In particular, it was known that the optical structures created via optical pumping nonlinearities in alkaline vapors will create a corresponding magnetization in the atomic ground states, which, under the experimental conditions used, could be analyzed in the framework of a spin-1/2 system, and the resulting structures corresponded to modulations of magnetic dipole moments [13,26–29]. In the meantime, an important research direction established in the atomic, molecular, and optical physics community is the simulation of complex quantum systems, e.g., from condensated matter physics, using well-controlled systems based on laser-cooled or quantum degenerate atomic samples. In particular, the investigation of classical and quantum magnetism is at the center of growing research using ultracold Bose and Fermi gases [30]. Effective exchange interactions have been studied in dilute Bose–Einstein condensates and degenerate Fermi gases at temperatures low enough to observe ferromagnetic or antiferromagnetic (AFM) coupling [31–36] including recent progress towards highly configurable simulators [37–41]. Hence it appears to be fruitful to look at self-organization in a coupled atom-light system to give rise not only to interactions between light waves, as in conventional nonlinear optics, but also to interactions between atoms leading to long-range atomic ordering. Effective long-range interaction between atoms is possible using transversely pumped cavities (see e.g., [42–47]). Furthermore, progress in optical trapping and cooling technology has enabled ensembles with high optical density to make single-mirror feedback and counterpropagating beam experiments feasible in cold atom setups [48–56]. As a first result on magnetic ordering, Ref. [56] connected magnetic dipole states in the Rb ground state to the transverse Ising model.

However, typically alkaline atoms possess a more complicated ground state, not only allowing for magnetic dipole moments (orientation) but also for higher multipoles such as, for example, magnetic quadrupoles (alignments). Contrary to the analogy between magnetic dipole structures and the Ising model [56], we are not aware of a specific Hamiltonian describing quadrupole dynamics in condensed matter to be simulated by a diffractive optical feedback scheme but note that recent interest in the community is directed towards investigations in higher-dimensional

spaces than offered by spin-1/2 systems, e.g., in the spin-1 Haldane model [57–59]. Additional interest stems from the fact that some alignment components represent optically induced coherences between Zeeman sublevels, related to quantum interference phenomena like coherent population trapping, electromagnetically induced transparency, and electromagnetically induced absorption [60–63]. There has been a significant interest in exploring spatially structured coherences for image storage for quantum information purposes [64–68]. Some theoretical papers considered the possibility of coherence-based self-organized states in cavities [69,70], but we are not aware of any experiment.

In this paper, we describe the observation of spontaneous spin structures due to light-mediated interaction in a cold thermal cloud. We investigate the rich three-dimensional phase diagram obtained when applying a weak magnetic field to the atoms and identify phases relying on both dipole and quadrupole moments of the atomic magnetization. In particular, we are reporting on the observation of spontaneous structures in ground-state coherences representing magnetic quadrupoles and where they occur in parameter space with respect to the dipole-based patterns.

2. PRINCIPLE OF EXPERIMENT

The present work builds on earlier experiments on the spontaneous emergence of ordered spatial structures, first in hot vapors [13,14,16], and then in cold atoms [49–52]. As demonstrated in Refs. [13,14,16], the nonlinear interaction between light and atoms can rely on the *magnetic* degrees of freedom.

To analyze our system, we expand the density matrix in the irreducible tensor basis, where the coefficients of the expansion give the magnetic multipole moments of the ensemble magnetization [71]. In the following, we describe the atom-light coupling using a $F = 1 \rightarrow F' = 2$ transition [see Fig. 1(a)]. This level structure is simpler than the $F = 2 \rightarrow F' = 3$ transition of the ^{87}Rb D2 line used in the experiment, but still presents components of the magnetic moment beyond the usual dipole. These components, illustrated in Fig. 1(a), are expressed in terms of density matrix elements ρ_{ij} in the Zeeman sublevel basis. The first moment is the monopole, given by the total population in the ground state, in our case equal to 1. The second moment is the spin orientation (dipole), with its z-direction component proportional to $w = \rho_{11} - \rho_{-1-1}$ (left). The orientation can be produced by Zeeman pumping with elliptically polarized light and is proportional to the expectation value of the magnetic dipole operator F_z [72]. The third moment is the quadrupole, with a total of five components, where only three couple directly to light in our model. The alignment $X = \rho_{11} + \rho_{-1-1} - 2\rho_{00}$ corresponds to a symmetric but uneven population distribution. It is obtained through Zeeman pumping with two circular fields with the same amplitude but opposite helicities (σ^+ and σ^-), corresponding, for example, to a linear polarization orthogonal to z. The two σ fields can also couple to the same excited state, as shown on the right of Fig. 1(a), to drive a Zeeman coherence between stretched states $\Phi = 2\rho_{1-1} = u + iv$. u and v correspond to quadrupole states in the (x, y) plane [71]. Alignment X and coherences u and v are also proportional to expectation values of the quadrupole hyperfine operators $3F_z^2 - F^2$, $F_x^2 - F_y^2$, and $F_xF_y + F_yF_x$, respectively [72].

Both orientation and alignment arise from incoherent processes described by rate equations. In contrast, the description of Zeeman coherences requires the use of optical Bloch equations. For $F' < F$ transitions, coherent processes lead to coherent population trapping [73] and electromagnetically induced transparency [61,68], and for $F' > F$ to electromagnetically induced absorption [62].

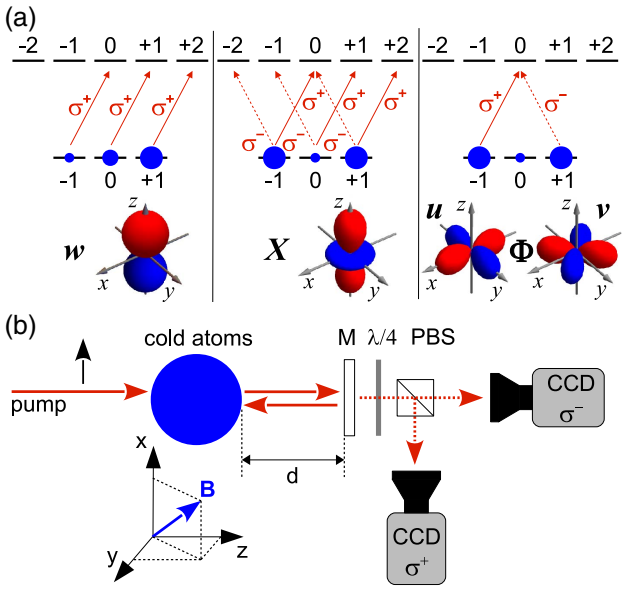

Fig. 1. Principle of experiment. (a) Components of magnetic moment and symmetries: orientation w (left, dipole), alignment X (middle, quadrupole), and coherence between stretched states $\Phi = u + iv$ (right, quadrupole). (b) Experimental setup. A detuned laser beam, linearly polarized along x, is sent through the cold cloud and retroreflected by a mirror (M). The transverse intensity distribution of the light is recorded in both circular polarization channels, using a quarter-wave plate ($\lambda/4$) + polarizing beam splitter (PBS) assembly.

The dispersive optical properties of the gas are determined by the medium polarization $\mathcal{P}_\pm$ induced by the circularly polarized fields $E_\pm$:

$$\mathcal{P}_\pm = \epsilon_0 \,\mathrm{Re}(\chi_\pm)\left[\left(1 \pm \frac{3}{4}w + \frac{1}{20}X\right)E_\pm + \frac{3}{20}(u \mp iv)E_\mp\right], \tag{1}$$

where $\mathrm{Re}(\chi_\pm) = \frac{\mathrm{OD}}{kL}\frac{2(\delta \mp \Omega_z)/\Gamma}{1+(2(\delta \mp \Omega_z)/\Gamma)^2}$ is the real part of the linear susceptibility (k is the wave vector, OD the cloud's optical density at resonance, L its thickness, δ the laser detuning, and Γ the atomic linewidth). Ω_z denotes the Zeeman shift in the presence of a longitudinal magnetic field B_z. The first term in Eq. (1) describes the phase shift experienced by the $\sigma^\pm$ fields, while the second one is a conversion term between σ^+ and σ^- in the presence of Φ. The dynamics of w, X, and Φ is governed by a set of coupled equations involving light and magnetic field (see Supplement 1). Thus, the structures discussed here are highly sensitive to both light polarization and magnetic field, in contrast with previous observations in cold atoms [51,52]. Their observation requires an adjustment of the experimental parameters as detailed below.

The experiment, sketched in Fig. 1(b), is based on the single-mirror feedback setup [9]. A large ($L = 1.4$ cm, OD ≈ 80, atom number $\approx 10^{11}$) and cold (≈ 200 μK) atomic cloud released from a magneto-optical trap is illuminated by a pulsed "pump" laser beam (pulse duration 400 μs) of waist 2.2 mm and peak intensity I_0 propagating along z and linearly polarized along x. This laser is

detuned from the atomic transition such that single-pass absorption is moderate (typically 20%), justifying the dispersive description of Eq. (1). The transmitted beam is retroreflected by a semitransparent mirror ($R > 99\%$) located at a distance d behind the cloud. An imaging optical system, not shown in the figure, is inserted between the atomic cloud and the mirror. It allows access to negative values of d, as demonstrated in Ref. [17]. A typical mechanism for self-organization is as follows. Consider a local, microscopic fluctuation of the orientation $w(x, y)$ resulting in a phase difference between transmitted σ^+ and σ^- fields. After diffractive propagation over $2d$, this phase difference turns into an intensity imbalance yielding a differential Zeeman pumping that enhances the initial orientation fluctuation. Above a certain intensity threshold, spontaneous symmetry breaking occurs, leading to the formation of two-dimensional spatial structures in the transverse plane for both light and orientation. The light transmitted by the mirror is used to image the transverse intensity distribution of the beam either in near field (NF) or in far field (FF). This imaging can be performed simultaneously in two orthogonal polarization channels, either circular (σ^+/σ^-) or linear (termed $\parallel$ and $\perp$ for a polarization aligned with that of the pump, or orthogonal to it).

By using cold atomic samples, Doppler effects are minimized, allowing for the clear observation of several different mechanisms leading to the formation of spatial structures [51,52]. We can select a specific mechanism by choosing the appropriate experimental parameters. To observe spin structures, we set the laser detuning at a negative value (typically $\delta = -8\Gamma$). Indeed, it was shown in Ref. [74] that only self-focusing nonlinearities support pattern formation in a thick medium, as self-focusing balances diffraction. This was indeed confirmed for an effectively two-level cold atomic system, where red detuned patterns were poorly contrasted compared to blue detuned ones [52]. When atoms are optically pumped toward stretched states, the refractive index increases (respectively decreases) for negative (respectively positive) detunings due to an increased effective Clebsch–Gordan coefficient. Hence the associated nonlinearity is self-focusing for $\delta < 0$, and magnetic patterns are only observed for red detuned light.

We use a laser intensity as low as 1 mW/cm^2, typically 2 orders of magnitude below the thresholds of these nonmagnetic instabilities. The excited state population is thus low ($\approx 10^{-3}$), and pattern formation is dominated by ground-state physics. We also cancel the residual magnetic field down to ≈10 mG in all three dimensions.

3. RESULTS AND DISCUSSION

We apply a control magnetic field and vary its direction and magnitude to observe the complex phase space reported in Fig. 2. Each phase is characterized by a specific spatial distribution of the light intensity and of the underlying atomic spins. We observe a phase with square symmetry (AFM, in red), localized around $B = 0$. Slightly increasing the longitudinal magnetic field B_z leads to an hexagonal phase (ferrimagnetic (FM), in blue). A larger B_z eventually produces a phase without long-range order, but with a local remaining hexagonal symmetry ("high B_z", in magenta). All these phases vanish when the transverse field (B_x or B_y) is increased [Figs. 2(a) and 2(b)]. However, a new disordered phase with a peculiar symmetry ("coherence," in green) appears when increasing B_x, the B-field component along the pump polarization, beyond a certain point [Fig. 2(b)].

This phase space depends on experimental parameters such as OD and laser intensity. Reducing the OD leads to the appearance of gaps between the AFM and coherence phases on one hand, and between the FM and high B_z phases on the other hand. Lowering the OD to 40 leads to the vanishing of the coherence phase. This proves that these phases are of a different nature, with different OD thresholds. Increasing I_0 leads to a broadening of all the features seen in Fig. 2, because the boundary for a given phase is typically determined by the balance between a Larmor and a Rabi frequency. For instance, Zeeman pumping is hampered by a transverse magnetic field inducing coherent coupling between Zeeman substates [56]. Increasing I_0 requires a proportional increase of the magnetic field to obtain the same steady-state population.

Orientation has the highest prefactor in Eq. (1) and is thus expected to dominate the formation of spin structures, at least for weak transverse magnetic fields. Indeed, a detailed theoretical analysis (beyond the scope of this paper) reveals that the sequence AFM → FM → high-B_z phase observed when increasing B_z can be understood considering only the w term in Eq. (1). However,

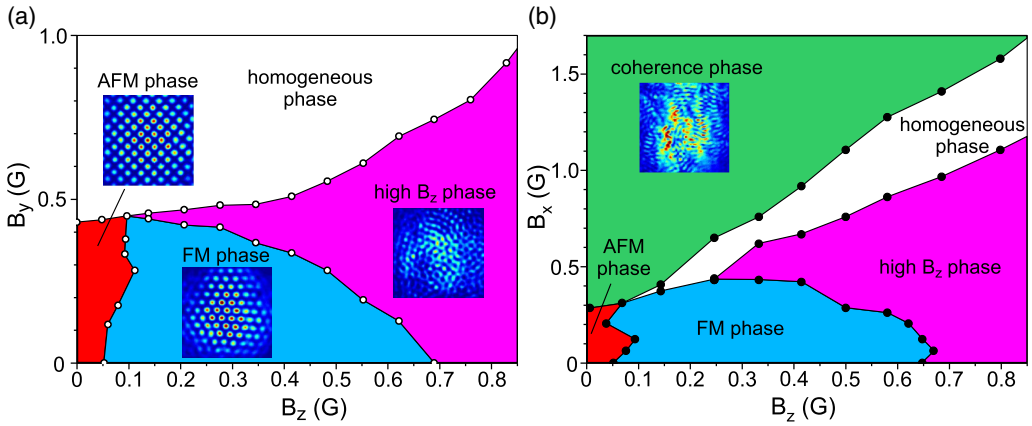

Fig. 2. Magnetic phase space of spin structures (experimental). Note that $B_x(B_y)$ is parallel (perpendicular) to the pump polarization axis. B_z is parallel to the pump propagation axis. (a) $B_y - B_z$ cross section of phase space. Three phases with different symmetries are observed as illustrated by NF images. These phases vanish for a large transverse field B_y. (b) $B_x - B_z$ cross section of phase space. An additional phase is observed when the transverse field B_x is increased. The structures typically take a few 10–100 μs to emerge and can persist for a few ms, suggesting that they are stable in the long term. Parameters: OD = 80, $I_0 = 8$ mW/cm^2, $\delta = -8\Gamma$, $d = -20$ mm.

the coupling of w to the other atomic quantities [75] needs to be retained in the analysis. We have also shown that the AFM and FM phases correspond, respectively, to antiferromagnetic and FM arrangements of atomic spin domains interacting via light. The transition to the homogeneous phase observed when increasing either B_x or B_y is due to the destruction of the orientation by the transverse field because of the coupling between Zeeman substates it induces. These findings, as well as analogies with the quantum Ising model, are discussed elsewhere [56].

We concentrate in the following on original spin phases that require the presence of quadrupole terms in the magnetic moment. This interesting physics extending beyond spin-1/2 models arises from our extended Zeeman structure. To promote these phases, we need to overcome the low coupling efficiencies associated with the X, u, and v terms in Eq. (1). This can be achieved by two means: increasing the transverse magnetic field to destroy orientation, or manipulating the effective interaction between spins by modifying the polarization of the feedback light.

We illustrate the first case in Fig. 3(a), where we plot the "diffracted power" P_d corresponding to the total power of the spatially modulated light extracted from the FF images as a function of $B_x(B_{y,z} = 0)$. P_d is recorded in both circular channels. The maximum at $B_x = 0$ corresponds to the orientation-based AFM phase of Fig. 2. Increasing $|B_x|$ leads to a rapid decrease of P_d and to the disappearance of the AFM phase around $|B_x| = 0.37$G. When $|B_x|$ is further increased, the coherence phase appears (shaded area). The amplitudes of the σ^+ and σ^- fields remain approximately equal, which is indeed expected for $B_z = 0$, as the Zeeman structure is symmetric [Fig. 1(a)]. We observe that the difference $\sigma^+ - \sigma^-$, which drives the growth of the orientation [75], does not show any spatial modulation in the coherence phase. It is, on the contrary, strongly modulated for the AFM, FM, and high B_z phases. For both phases of Fig. 3(a), most of the spatially modulated light is generated in the $\perp$ channel (polarization instability). This can be understood by looking at Eq. (1). The terms with $\pm$ or $\mp$ signs in front (w and v) yield a different optical response for σ^+ and σ^- fields and can thus change the polarization. On the opposite, X and u terms yield the same response to σ^+ and σ^- and hence do not modify the polarization.

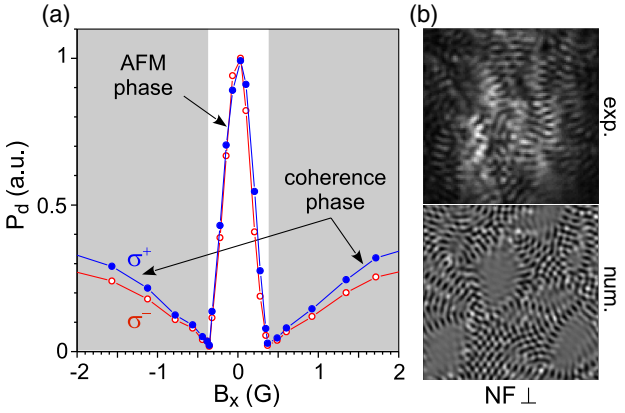

Fig. 3. Coherence phase. (a) B_x scan showing the transition from the AFM phase (white background) to the coherence phase (shaded). Parameters, $B_y = B_z = 0$; $I_0 = 12$ mW/cm^2; $\delta = -8\Gamma$; $d = -20$ mm; (b) experimental (top) and numerical (bottom) NF patterns for $B_x = 1$G, both in the $\perp$ channel. The field of view of the experimental image is 3.3 mm; the typical pattern length scale is 170 μm.

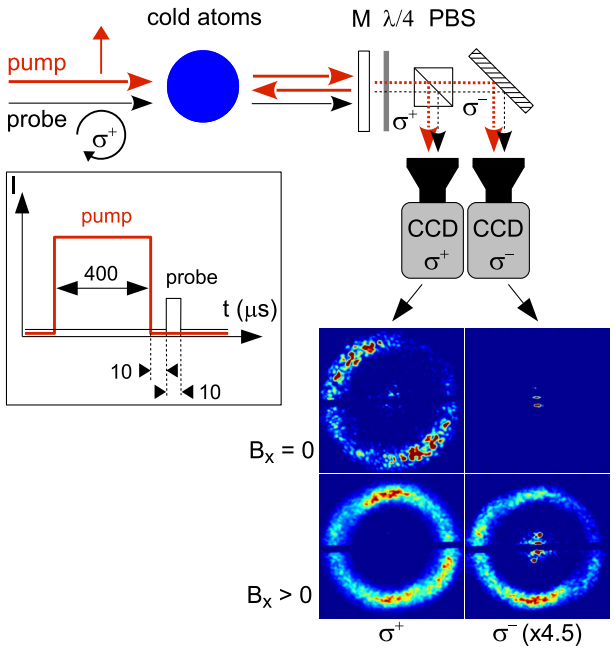

Fig. 4. Experimental evidence for a strong spatial modulation of Φ in the coherence phase. A σ^+ weak probe is sent through the cloud shortly after the pump, and FF images are detected in the σ^+ and σ^- channels. For $B_x = 0$, all the spatially modulated probe light is detected in σ^+. On the contrary, for $B_x = 1.5$G, approximately 20% of the spatially modulated probe light is transferred to the σ^- channel.

These observations suggest that v is responsible for the coherence phase. To confirm this hypothesis, we performed the experimental test illustrated in Fig. 4. Immediately after the pump pulse, we sent a much weaker probe pulse of σ^+ polarization. If a spatially modulated coherence is present and provides a "cross-channel" gain between σ^+ and σ^-, we expect some sizable amount of light to be transferred to the σ^- channel. This was indeed observed for $B_x = 1.5$G, with up to 20% of spatially modulated probe light detected in the σ^- channel. For $B_x = 0$, the detected amount was negligible. This observation proves that a large spatial modulation of Φ is present when the structures shown in Fig. 3(b) are observed. Our numerical simulations indeed confirm the existence of an instability at large B_x, associated with a spatial modulation of v 1 order of magnitude larger than observed for $B = 0$. The numerical patterns displayed in Fig. 3(b) (bottom) are qualitatively rather similar to those observed in the experiment [Fig. 3(b), top]: in particular, the peculiar arrangement of these structures with patches, sinuous lines of defects, and a lack of clear global symmetry is well reproduced. We stress that a quantitative agreement is beyond our present simulation capabilities, both because of our simplified transition model and the fact that thick-medium effects [74] are neglected. The simulations, however, allow direct access to the atomic states [75]. Our analysis shows that the linearly polarized pump beam only creates the u component of the coherence, which corresponds to a quadrupole aligned along the x and y axes [Fig. 1(a), right column]. The instability creates a v component with a spatially modulated amplitude (the amplitude of u being modulated as well). The result is a state with a quadrupole moment of spatially modulated amplitude, and whose axes are oscillating in space around the x and y axes. In optical terms, this corresponds

to a coherence Φ, whose amplitude and phase are spatially modulated.

As mentioned above, the phases observed around $B = 0$ are essentially orientation-based. In principle, the structure of our ground state can also support a modulated alignment $X(x, y)$, with an associated novel phase. An X-based instability is, however, not favored according to Eq. (1) because of its small prefactor. As alignment is as sensitive to transverse B fields as orientation, we need to selectively suppress the orientation mechanism at $B = 0$. To this end, we inserted inside the feedback loop a polarizing beam-splitter (PBS) aligned to transmit the pump polarization [Fig. 5(a)]. By imposing a polarization-maintaining feedback, we aim at suppressing the w-based instability (and any polarization instability, for that matter). On the contrary, we expect an X instability to remain unaffected, since the alignment term cannot sustain a polarization instability. We detect the spatially modulated light both in the ∥ channel (transmitted by the PBS and the mirror) and in the ⊥ channel (now rejected by the PBS). The FF images in Figs. 5(b) and 5(c) show that spatial structures are observed in both polarization channels. In the plots of Figs. 5(b) and 5(c), we record the transverse wave vector q of the diffracted light as a function of the feedback distance d. A variation of q with d is a signature of mirror feedback [9]. We observe that in the ∥ channel [Fig. 5(c)] the mirror feedback is still operational: q varies with d. A polarization-preserving mechanism is thus at work, which from the previous discussion can only involve X or u. We observed that the intensity threshold of this instability is higher by a factor of 3 than that of the w instability (in the absence of PBS inside the feedback loop). The structures vanish if we increase the transverse magnetic field B_x. These observations appear to be consistent with a role played by the alignment. A mechanism based on the u term seems unlikely, since the role of the coherence Φ is favored by B_x (Fig. 3). Surprisingly, we also observe patterns in the ⊥ channel, but with a *d-independent* wave vector [Fig. 5(b)]. Indeed, due to the large thickness of our atomic cloud, diffraction takes place inside the cloud, and we can observe instabilities using two "independent" counterpropagating beams instead of a retroreflected one [53]. In this situation, the wave vector of the instability is determined by the cloud's thickness L and is independent of d. We thus conjecture that two instabilities coexist in the presence of the PBS inside the feedback loop: an alignment-based instability (without polarization instability) with mirror feedback in the ∥ channel, and an orientation-based instability (with polarization instability) without mirror feedback in the ⊥ channel. This unprecedented and complicated situation obviously requires more investigation, since thick-medium effects [74] have to be included in the theoretical analysis.

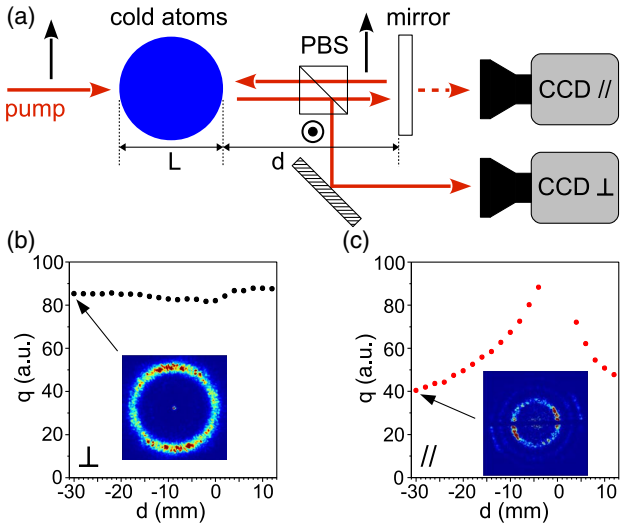

Fig. 5. Alignment phase. (a) Modified setup with a PBS inside the feedback loop. We monitor the wave vector q of the spatial structures versus feedback distance d in both ∥ and ⊥ polarization channels. (b) q versus d in the ⊥ channel. q is nearly d-independent (no mirror feedback). (c) q versus d in the ∥ channel. Active mirror feedback hints at a polarization-preserving instability mechanism. $B = 0$, $I_0 = 53$ mW/cm^2, $\delta = -8\Gamma$.

4. CONCLUSION

In conclusion, we investigated the spontaneous formation of spatial spin structures in a cold atomic cloud submitted to optical feedback. This system, coherently driven and dissipative [76], displays an unconventional form of magnetism where atomic spins interact nonlocally via light. It offers the possibility to tailor effective spin-spin interactions through modifications of the feedback loop. By tuning a weak magnetic field, we induced transitions between phases with various symmetries relying on the spatial modulation of different components of the atomic magnetic moment, corresponding to both dipole and quadrupole terms. In particular, we observed an original phase based on ground-state Zeeman coherences, which was not accessible in previous spin-1/2 studies. This could spark a renewed interest in the quest to store spatial information in atomic coherences for quantum memories [64–68]. Future directions include the investigation of other atomic transitions, the statistics of symmetry breaking and Kibble–Zurek dynamics [53], the influence of frustration, and the search for optically controllable localized magnetic structures. We also plan to investigate the interplay between magnetic and optomechanical [51] self-organization. At much higher densities, additional effects due to long range dipole-dipole interactions could also be studied.

Funding. Leverhulme Trust; University of Strathclyde; Centre National de la Recherche Scientifique (CNRS); Université Nice Sophia Antipolis (UNS); Région Provence-Alpes-Côte d'Azur; Royal Society; Horizon 2020 Framework Programme (H2020); Hrvatska Zaklada za Znanost (HRZZ) (IP-2014-09-7342).

Acknowledgment. The Strathclyde group is grateful for support from the Leverhulme Trust. IK gratefully acknowledges a University Studentship from the University of Strathclyde. The Nice group acknowledges support from CNRS, UNS, and Région PACA. The collaboration between the two groups was supported by the Royal Society (London), CNRS, and in particular, the Laboratoire International Associé "Solace," and the Global Engagement Fund of the University of Strathclyde. The final stage of this work was performed in the framework of the European Training network ColOpt, which is funded by the European Union Horizon 2020 program under the Marie Skłodowska-Curie action.

See Supplement 1 for supporting content.

REFERENCES AND NOTES

1. G. Grynberg, E. Le Bihan, P. Verkerk, P. Simoneau, J. R. R. Leite, D. Bloch, S. Le Boiteux, and M. Ducloy, "Observation of instabilities due to mirrorless four-wave mixing oscillation in sodium," Opt. Commun. **67**, 363–366 (1988).
2. L. A. Lugiato and R. Lefever, "Spatial dissipative structures in passive optical systems," Phys. Rev. Lett. **58**, 2209–2211 (1987).
3. M. Kreuzer, H. Gottschilk, T. Tschudi, and R. Neubecker, "Structure formation and self-organization phenomena in bistable optical elements," Mol. Cryst. Liq. Cryst. **207**, 219–230 (1991).
4. J. B. Geddes, J. V. Moloney, E. M. Wright, and W. J. Firth, "Polarization patterns in a nonlinear cavity," Opt. Commun. **111**, 623–631 (1994).
5. A. J. Scroggie, W. J. Firth, G. S. McDonald, M. Tlidi, R. Lefever, and L. A. Lugiato, "Pattern formation in a passive Kerr cavity," Chaos Solitons Fractals **4**, 1323–1354 (1994).
6. M. Tlidi and P. Mandel, "Localized structures and localized patterns in optical bistability," Chaos Solitons Fractals **4**, 1475–1486 (1994).
7. G.-L. Oppo, M. Brambilla, and L. A. Lugiato, "Formation and evolution of roll patterns in optical parametric oscillators," Phys. Rev. A **49**, 2028–2032 (1994).
8. R. Kuszelewicz, I. Ganne, I. Sagnes, and G. Slekys, "Optical self-organization in bulk and multiquantum well GaAlAs microresonators," Phys. Rev. Lett. **84**, 6006–6009 (2000).
9. W. J. Firth, A. Fitzgerald, and C. Pare, "Transverse instabilities due to counterpropagation in Kerr media," J. Opt. Soc. Am. B **7**, 1087–1097 (1990).
10. G. D'Alessandro and W. J. Firth, "Spontaneous hexagon formation in a nonlinear optical medium with feedback mirror," Phys. Rev. Lett. **66**, 2597–2600 (1991).
11. R. Macdonald and H. J. Eichler, "Spontaneous optical pattern formation in a nematic liquid crystal with feedback mirror," Opt. Commun. **89**, 289–295 (1992).
12. T. Honda, "Hexagonal pattern formation due to counterpropagation in $KNbO_3$," Opt. Lett. **18**, 598–600 (1993).
13. G. Grynberg, A. Maître, and A. Petrossian, "Flowerlike patterns generated by a laser beam transmitted through a rubidium cell with a single feedback mirror," Phys. Rev. Lett. **72**, 2379–2382 (1994).
14. T. Ackemann and W. Lange, "Non- and nearly hexagonal patterns in sodium vapor generated by single-mirror feedback," Phys. Rev. A **50**, R4468–R4471 (1994).
15. M. Schwab, M. Sedlatschek, B. Thüring, C. Denz, and T. Tschudi, "Origin and control of dynamics of hexagonal patterns in a photorefractive feedback system," Chaos Solitons Fractals **10**, 701–707 (1999).
16. A. Aumann, E. Büthe, Y. Logvin, T. Ackemann, and W. Lange, "Polarized patterns in sodium vapor with single mirror feedback," Phys. Rev. A **56**, R1709–R1712 (1997).
17. E. Ciaramella, M. Tamburrini, and E. Santamato, "Talbot assisted hexagonal beam patterning in a thin liquid crystal film with a single feedback mirror at negative distance," Appl. Phys. Lett. **63**, 1604–1606 (1993).
18. G. Grynberg, "Mirrorless four-wave mixing oscillation in atomic vapors," Opt. Commun. **66**, 321–324 (1988).
19. J. Pender and L. Hesselink, "Degenerate conical emissions in atomic-sodium vapor," J. Opt. Soc. Am. B **7**, 1361–1373 (1990).
20. D. J. Gauthier, M. S. Malcuit, A. L. Gaeta, and R. W. Boyd, "Polarization bistability of counterpropagating laser beams," Phys. Rev. Lett. **64**, 1721–1724 (1990).
21. A. Petrossian, M. Pinard, A. Maître, J. Y. Courtois, and G. Grynberg, "Transverse pattern formation for counterpropagating laser beams in rubidium vapour," Europhys. Lett. **18**, 689–695 (1992).
22. A. M. C. Dawes, L. Illing, S. M. Clark, and D. J. Gauthier, "All-optical switching in rubidium vapor," Science **308**, 672–674 (2005).
23. S. A. Akhmanov, M. A. Vorontsov, and V. Y. Ivanov, "Large-scale transverse nonlinear interactions in laser beams; new types of nonlinear waves; onset of 'optical turbulence'," JETP Lett. **47**, 707–710 (1988).
24. E. Pampaloni, S. Residori, and F. T. Arecchi, "Roll-hexagon transition in a Kerr-like experiment," Europhys. Lett. **24**, 647–652 (1993).
25. B. Thüring, R. Neubecker, and T. Tschudi, "Transverse pattern formation in liquid crystal light valve feedback system," Opt. Commun. **102**, 111–115 (1993).
26. G. Grynberg, "Drift instability and light-induced spin waves in an alkali vapor with a feedback mirror," Opt. Commun. **109**, 483–486 (1994).
27. T. Ackemann, Y. A. Logvin, A. Heuer, and W. Lange, "Transition between positive and negative hexagons in optical pattern formation," Phys. Rev. Lett. **75**, 3450–3453 (1995).
28. M. Le Berre, D. Leduc, E. Ressayre, A. Tallet, and A. Maître, "Simulation and analysis of the flower-like instability in the single-feedback mirror experiment with rubidium vapor," Opt. Commun. **118**, 447–456 (1995).
29. A. J. Scroggie and W. J. Firth, "Pattern formation in an alkali-metal vapor with a feedback mirror," Phys. Rev. A **53**, 2752–2764 (1996).
30. C. Gross and I. Bloch, "Quantum simulations with ultracold atoms in optical lattices," Science **357**, 995–1001 (2017).
31. J. Stenger, S. Inouye, D. Stamper-Kurn, H.-J. Miesner, A. Chikkatur, and W. Ketterle, "Spin domains in ground-state Bose–Einstein condensates," Nature **396**, 345–348 (1998).
32. M.-S. Chang, C. D. Hamley, M. D. Barrett, J. A. Sauer, K. M. Fortier, W. Zhang, L. You, and M. S. Chapman, "Observation of spinor dynamics in optically trapped ^{87}Rb Bose–Einstein condensates," Phys. Rev. Lett. **92**, 140403 (2004).
33. M. Vengalattore, S. R. Leslie, J. Guzman, and D. M. Stamper-Kurn, "Spontaneously modulated spin textures in a dipolar spinor Bose–Einstein condensate," Phys. Rev. Lett. **100**, 170403 (2008).
34. J. Kronjäger, C. Becker, P. Soltan-Panahi, K. Bongs, and K. Sengstock, "Spontaneous pattern formation in an antiferromagnetic quantum gas," Phys. Rev. Lett. **105**, 090402 (2010).
35. D. Jacob, L. Shao, V. Corre, T. Zibold, L. De Sarlo, E. Mimoun, J. Dalibard, and F. Gerbier, "Phase diagram of spin-1 antiferromagnetic Bose–Einstein condensates," Phys. Rev. A **86**, 061601 (2012).
36. D. Greif, T. Uehlinger, G. Jotzu, L. Tarruel, and T. Esslinger, "Short-range quantum magnetism of ultracold fermions in an optical lattice," Science **340**, 1307–1310 (2013).
37. J. Stuhler, A. Griesmaier, T. Koch, M. Fattori, T. Pfau, S. Giovanazzi, P. Pedri, and L. Santos, "Observation of dipole-dipole interaction in a degenerate quantum gas," Phys. Rev. Lett. **95**, 150406 (2005).
38. H. Kadau, M. Schmitt, M. Wenzel, C. Wink, T. Maier, I. Ferrier-Barbut, and T. Pfau, "Observing the Rosensweig instability of a quantum ferrofluid," Nature **530**, 194–197 (2016).
39. H. Labuhn, D. Barredo, S. Ravets, S. de Léséleuc, T. Macr, T. Lahaye, and A. Browaeys, "Tunable two-dimensional arrays of single Rydberg atoms for realizing quantum Ising models," Nature **534**, 667–670 (2016).
40. J. Zeiher, J.-Y. Choi, A. Rubio-Abadal, T. Pohl, R. van Bijnen, I. Bloch, and C. Gross, "Coherent many-body spin dynamics in a long-range interacting Ising chain," Phys. Rev. X **7**, 041063 (2017).
41. H. Bernien, S. Schwartz, A. Keesling, H. Levine, A. Omran, H. Pichler, S. Choi, A. S. Zibrov, M. Endres, M. Greiner, V. Vuletić, and M. D. Lukin, "Probing many-body dynamics on a 51-atom quantum simulator," Nature **551**, 579–584 (2017).
42. P. Domokos and H. Ritsch, "Collective cooling and self-organization of atoms in a cavity," Phys. Rev. Lett. **89**, 253003 (2002).
43. A. T. Black, H. W. Chan, and V. Vuletic, "Observation of collective friction forces due to spatial self-organization of atoms: from Rayleigh to Bragg scattering," Phys. Rev. Lett. **91**, 203001 (2003).
44. K. Baumann, C. Guerlin, F. Brennecke, and T. Esslinger, "Dicke quantum phase transition with a superfluid gas in an optical cavity," Nature **464**, 1301–1306 (2010).
45. A. J. Kollar, A. T. Papageorge, V. D. Vaidya, Y. Guo, J. Keeling, and B. L. Lev, "Supermode-density-wave-polariton condensation with a Bose–Einstein condensate in a multimode cavity," Nat. Commun. **8**, 14386 (2017).
46. J. Léonard, A. Morales, P. Zupancic, T. Esslinger, and T. Donner, "Supersolid formation in a quantum gas breaking a continuous translational symmetry," Nature **543**, 87–90 (2017).
47. M. Landini, N. Dogra, K. Kroeger, L. Hruby, T. Donner, and T. Esslinger, "Formation of a spin texture in a quantum gas coupled to a cavity," Phys. Rev. Lett. **120**, 223602 (2018).
48. J. A. Greenberg, B. L. Schmittberger, and D. Gauthier, "Bunching-induced optical nonlinearity and instability in cold atoms," Opt. Express **19**, 22535–22549 (2011).
49. J. A. Greenberg and D. J. Gauthier, "Steady-state, cavityless, multimode superradiance in a cold vapor," Phys. Rev. A **86**, 013823 (2012).
50. J. A. Greenberg and D. J. Gauthier, "High-order optical nonlinearity at low light levels," Europhys. Lett. **98**, 24001 (2012).
51. G. Labeyrie, E. Tesio, P. M. Gomes, G.-L. Oppo, W. J. Firth, G. R. M. Robb, A. S. Arnold, R. Kaiser, and T. Ackemann, "Optomechanical self-structuring in a cold atomic gas," Nat. Photonics **8**, 321–325 (2014).

52. A. Camara, R. Kaiser, G. Labeyrie, W. J. Firth, G.-L. Oppo, G. R. M. Robb, A. S. Arnold, and T. Ackemann, "Optical pattern formation with a two-level nonlinearity," Phys. Rev. A **92**, 013820 (2015).
53. G. Labeyrie and R. Kaiser, "Kibble–Zurek mechanism in the self-organization of a cold atomic cloud," Phys. Rev. Lett. **117**, 275701 (2016).
54. B. L. Schmittberger and D. J. Gauthier, "Spontaneous emergence of free-space optical and atomic patterns," New J. Phys. **18**, 103021 (2016).
55. B. L. Schmittberger and D. J. Gauthier, "Transverse optical and atomic pattern formation," J. Opt. Soc. Am. B **33**, 1543–1551 (2016).
56. I. Kresic, G. Labeyrie, G. R. M. Robb, G.-L. Oppo, P. M. Gomes, P. Griffin, R. Kaiser, and T. Ackemann, "Spontaneous light-mediated magnetism in cold atoms," Commun. Phys. **1**, 33 (2018).
57. C. Senko, P. Richerme, J. Smith, A. Lee, I. Cohen, A. Retzker, and C. Monroe, "Realization of a quantum integer-spin chain with controllable interactions," Phys. Rev. X **5**, 021026 (2015).
58. Z.-X. Gong, M. F. Maghrebi, A. Hu, M. Foss-Feig, P. Richerme, C. Monroe, and A. V. Gorshkov, "Kaleidoscope of quantum phases in a long-range interacting spin-1 chain," Phys. Rev. B **93**, 205115 (2016).
59. H. J. Lee, M. Choi, and G. S. Jeon, "Emergent incommensurate correlations in frustrated ferromagnetic spin-1 chains," Phys. Rev. B **95**, 024424 (2017).
60. E. Arimondo and G. Orriols, "Nonabsorbing atomic coherences by coherent two-photon transitions in a three-level optical pumping," Lett. Nuovo Cimento **17**, 333–338 (1976).
61. K.-J. Boller, A. Imamoglu, and S. E. Harris, "Observation of electromagnetically induced transparency," Phys. Rev. Lett. **66**, 2593–2596 (1991).
62. A. M. Akulshin, S. Barreiro, and A. Lezama, "Electromagnetically induced absorption and transparency due to resonant two-field excitation of quasidegenerate levels in Rb vapor," Phys. Rev. A **57**, 2996–3002 (1998).
63. M. Fleischhauer, A. Imamoglu, and J. P. Marangos, "Electromagnetically induced transparency: optics in coherent media," Rev. Mod. Phys. **77**, 633–673 (2005).
64. P. K. Vudyasetu, R. M. Camacho, and J. C. Howell, "Storage and retrieval of multimode transverse images in hot atomic rubidium vapor," Phys. Rev. Lett. **100**, 123903 (2008).
65. M. Shuker, O. Firstenberg, R. Pugatch, A. Ron, and N. Davidson, "Storing images in warm atomic vapor," Phys. Rev. Lett. **100**, 223601 (2008).
66. G. Heinze, C. Hubrich, and T. Halfmann, "Stopped light and image storage by electromagnetically induced transparency up to the regime of one minute," Phys. Rev. Lett. **111**, 033601 (2013).
67. D.-S. Ding, Z.-Y. Zhou, B.-S. Shi, and G.-C. Guo, "Single-photon-level quantum image memory based on cold atomic ensembles," Nat. Commun. **4**, 2527 (2013).
68. N. Radwell, T. W. Clark, B. Piccirillo, S. M. Barnett, and S. Franke-Arnold, "Spatially dependent electromagnetically induced transparency," Phys. Rev. Lett. **114**, 123603 (2015).
69. G.-L. Oppo, "Complex spatial structures due to atomic coherence," J. Mod. Opt. **57**, 1408–1416 (2010).
70. M. Eslami, R. Kheradmand, D. McArthur, and G.-L. Oppo, "Complex structures in media displaying electromagnetically induced transparency: pattern multistability and competition," Phys. Rev. A **90**, 023840 (2014).
71. M. Auzinsh, D. Budker, and S. Rochester, *Optically Polarized Atoms: Understanding Light-Atom Interactions* (Oxford University, 2010).
72. A. Omont, "Irreducible components of the density matrix. Application to optical pumping," Prog. Quantum Electron. **5**, 69–138 (1977).
73. A. Aspect, E. Arimondo, R. Kaiser, N. Vansteenkiste, and C. Cohen-Tannoudji, "Laser cooling below the one-photon recoil energy by velocity-selective coherent population trapping," Phys. Rev. Lett. **61**, 826–829 (1988).
74. W. J. Firth, I. Kresic, G. Labeyrie, A. Camara, and T. Ackemann, "Thick-medium model of transverse pattern formation in optically excited cold two-level atoms with a feedback mirror," Phys. Rev. A **96**, 053806 (2017).
75. See Supplement 1
76. E. M. Kessler, G. Giedke, A. Imamoglu, S. F. Yelin, M. D. Lukin, and J. I. Cirac, "Dissipative phase transition in a central spin system," Phys. Rev. A **86**, 012116 (2012).